COMMUNICATION

Does the energy transfer from Ar(1s) atoms to N_2 lead to dissociation?

Claus-Peter Klages[1] 🔗 | **Andris Martinovs[1]** | **Lars Bröcker[1]** 🔗 | **Detlef Loffhagen[2]** 🔗

[1]Institute for Surface Technology, IOT, Technische Universität Braunschweig, Braunschweig, Germany

[2]Department of Plasma Modelling, Leibniz Institute for Plasma Science and Technology (INP), Greifswald, Germany

Correspondence
Claus-Peter Klages, Institute for Surface Technology, IOT, Technische Universität Braunschweig, Bienroder Weg 54 E, 38108 Braunschweig, Germany.
Email: c-p.klages@tu-braunschweig.de

Abstract

Dielectric-barrier discharges (DBDs) in Ar–N_2 mixtures, with N_2 fractions in 0.1–1% range, would be attractive alternatives to DBDs in pure N_2 if energy-transfer reactions between Ar(1s) atoms and N_2 molecules were an efficient source of N atoms. Attempts to functionalize polyolefins in flowing post-discharges fed by such DBDs, as well as the search for the First Positive System in the emission spectrum, however, failed. Evidently, the energy-transfer reactions do not produce N atoms. For Ar($1s_3$) and Ar($1s_5$) metastable states, this fact has already been reported in the literature. For Ar($1s_2$) and Ar($1s_4$) resonant states, a quantitative argument is derived in this paper: energy transfer from Ar(1s) atoms to N_2 molecules is not an effi-
cient source of N atoms.

$$Ar(1s_i) + N_2(X) \xrightarrow{\;?\;} Ar(1p_0) + N(^4S) + N(^4S)$$
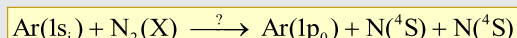
KEYWORDS

argon, dissociation, energy transfer, nitrogen

1 | INTRODUCTION

The dissociation of O_2 in a low-temperature, non-equilibrium plasma such as a dielectric-barrier discharge (DBD), the basis of the ozone production method found by W. Siemens in 1857, is highly energy-efficient, utilizing about 80% of the electron energy over a fairly wide range of reduced electric fields.[1] The corresponding process in molecular nitrogen, however, is energetically very costly: the dissociation of N_2 in DBDs in pure atmospheric pressure N_2 requires several hundreds of eV of electrical energy input for one N atom,[2,3] whereas the energy necessary to dissociate N_2 into two ground-state N atoms, D_{N_2}, is only 9.76 eV.[4] A large fraction of the energy dissipated in N_2 plasmas at reduced fields, typical of DBDs, goes into vibrationally excited states.[5] Adverse consequences are comparably high voltages necessary to

drive N_2 DBDs and excessive (vibrational) heating of the gas.

Therefore, in the course of studies on polymer surface modification in flowing nitrogen postdischarges ("afterglows") fed by DBDs, the authors spent substantial time attempting to provide ground-state nitrogen atoms, N(^4S), by utilizing energy transfer-based dissociation reactions in Ar–N_2 mixtures with small amounts of N_2 (molar fractions x_{N_2} below 1%):

$$Ar(1s_i) + N_2(X) \rightarrow Ar(1p_0) + N(^4S) + N(^4S), \quad (R1)$$
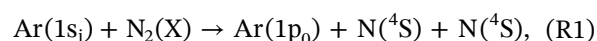
while largely avoiding excitation of molecular vibrations.

Species Ar($1s_i$) in R1 is an Ar atom in one of the four excited states with the electron configuration $1s^2 2s^2 2p^6 3s^2 3p^5 4s^1$, and Ar($1p_0$) is a a ground-state Ar atom. In Table 1, names and energies of these states, together with

TABLE 1   The four lowest energy excited states of argon and the triplet Ar_2 excimer

Racah notation	$4s(^3P_2)$	$4s(^3P_1)$	$4s(^3P_0)$	$4s(^1P_1)$	$Ar_2(^3\Sigma_u^+)$	Reference
Paschen notation	$1s_5$	$1s_4$	$1s_3$	$1s_2$	$-$[a]	
Energy/eV	11.55	11.62	11.72	11.83	9.8	[6,7]
$k_{Q,N_2}/10^{-11}$ cm^3/s	3.6	0.8	1.6	5.4	0.33	[8,9]

[a]In the following, "species numbers" $i = 2$ to 5 are attributed to $Ar(1s_{2,3,4,5})$, and $i = 6$ is attributed to the excimer, for clarity.

those of the excimer $Ar_2(^3\Sigma_u^+)$, are compiled. In this communication, the Paschen notation is used.

Reaction(s) R1 can be found in several papers, published in the recent 15 years, in which numerical modeling of plasmas in Ar–N_2 or Ar–air mixtures using plasma-chemical reaction models is reported.[10–16] In these models, either a single reaction R1 is used, with an unspecified excited species "Ar*" or the lowest energy metastable $Ar(1s_5)$ representing the species $Ar(1s_i)$ on the left-hand side of R1,[10,11,13,16] or two reactions are included, with species "Ar_m" and "Ar_r" denoting an Ar atom in a metastable and a resonant state, respectively.[12,15] In one paper, all four excited states are taken into account.[14] The reference for these reactions is—or it can be traced back to—the paper by Piper et al.,[17] in which rate coefficient k_Q for quenching of $Ar(1s_5)$ and $Ar(1s_3)$ by several small molecules is reported. The values for N_2 are given in Table 1.

If these reactions would actually proceed with the reported rate coefficients—1.6×10^{-11} cm^3/s[10,12,13,15,16] or 3.6×10^{-11} cm^3/s [11,14]—the dissociation of nitrogen using a DBD in an Ar–N_2 mixture, with an N_2 fraction of $x_{N_2} = 0.1–1\%$, would be an attractive alternative to a DBD in N_2, because N atoms could be produced at much smaller energy costs. As one can calculate from data given, for example, in a paper by Pitchford et al.,[18] an Ar DBD driven with a power density of 1 W/cm^3 should produce, at a typical reduced field strength of 100 Td, excited Ar atoms in 1s states with a total generation rate, g, of 4.4×10^{17} cm^{-3}/s, corresponding to an energy efficiency of about 80%. The same value results from the solution of the stationary electron Boltzmann equation.[19] With a rate coefficient for reaction R1, k_1, in the order of 10^{-11} cm^3/s, N_2 fractions in 0.1–1% range would be sufficient to utilize a major fraction of the $Ar(1s)$ atoms in energy-transfer reactions. The corresponding experiments conducted at IOT using afterglows from DBDs with $x_{N_2} = 0.1–1\%$, however, failed. It was not possible to achieve the expected surface modification of polyolefin surfaces, as it was observed with flowing post-discharges fed by DBDs in N_2; however, a substantial share of $Ar(1s)$ atoms should have reacted with N_2, resulting in dissociation. The failure of repeated attempts was the reason to take a closer look at the validity of reaction R1.

A first objection against a major role played by reactions R1, involving metastable Ar atoms, $Ar(1s_3)$ or $Ar(1s_5)$,

can be based on papers published by Setser et al.[20] already in the 1970s, showing that two excited states of molecular nitrogen, $N_2(C)$ and $N_2(B)$, are the only product of the quenching reactions of $Ar(1s_3)$ and $Ar(1s_5)$ with N_2. The authors noted explicitly that they were unable to detect N atoms in this system.[20] Main results were redetermined in 1977 and a branching ratio for $N_2(C)/N_2(B)$ of 1.0 ± 0.2 was found, using a 7:1 ratio of $Ar(1s_5)$ to $Ar(1s_3)$.[21]

However, an important question, whether atoms in resonant states, $Ar(1s_4)$ and $Ar(1s_2)$, are capable of dissociating N_2, remains unanswered. In typical Ar DBDs at atmospheric pressure, Ar atoms in the $1s_2$ or $1s_4$ state have a substantially higher average density than metastable $Ar(1s_5)$ atoms, owing to fast excimer formation from the latter in three-body reactions with two ground-state Ar atoms.[22]

2 | PERIOD-AVERAGED $Ar(1s)$ SPECIES DENSITIES $n_{Ar(1s_i)}$ AND QUENCHING RATES Q_i

Densities of different $Ar(1s)$ species in Ar–N_2 DBDs, time-averaged over the period of the excitation voltage, can be calculated using a facile analytical method, which was used earlier for plasma polymerization from Ar-monomer DBDs.[22] The method is based on a reaction kinetic model for generation and decay processes of the individual $Ar(1s)$ species and two excimers, $Ar_2(^3\Sigma_u^+)$ and $Ar_2(^1\Sigma_u^+)$,[23] including reactions with an added atomic or molecular species. Literature data are used for the total generation rate, $g = \Sigma_i\ g_i$, of $Ar(1s_i)$ states ($2 \leq i \leq 5$) due to direct excitation from the ground state and cascading from higher energetic states, and the shares of individual $Ar(1s_i)$ states, g_i.[18] Rate coefficients for quenching reactions of $Ar(1s)$ atoms with N_2, k_{Q,N_2}, given in Table 1, are taken from a paper by Velazco et al.,[8] and references cited therein. The corresponding rate coefficient for the excimer $Ar_2(^3\Sigma_u^+)$, formed in three-body collisions of $Ar(1s_5)$ with two ground-state Ar atoms[1] is taken from Reference [9]. Figure 1 shows

---

[1]The excimer $Ar_2(^1\Sigma_u^+)$, however, is virtually not quenched by N_2 under the relevant conditions, as it has a very short radiative lifetime (4 ns). It represents, however, a loss channel for $Ar(1s_4)$.
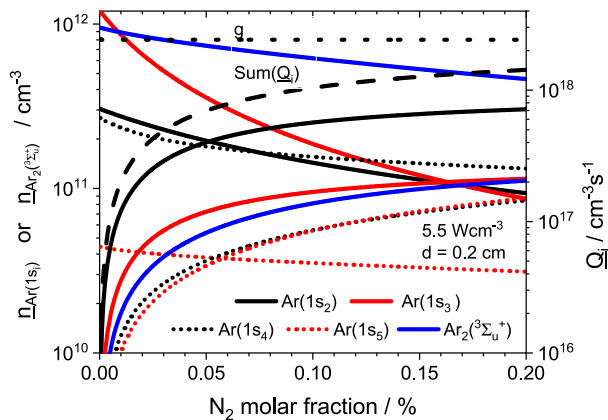
FIGURE 1 Period-averaged densities of Ar atoms in $1s_i$ states and excimers $Ar_2(^3\Sigma_u^+)$, respectively (descending curves), and average rate $\underline{Q}_i$ of individual quenching reactions of these species with N_2 (ascending curves) as a function of the N_2 content. The sum of $\underline{Q}_i$ ($i = 2$ to 5 for the $Ar(1s_i)$ states and $i = 6$ for the excimer) is represented by the dashed ascending curve; the dotted line is the total $Ar(1s)$ generation rate, g. The calculation was made for 5.5-W/cm^3 power density and 0.2-cm gap width

results of a calculation for a power density of 5.5 W/cm^3 and a gap width of 0.2 cm.

It shows that, in contrast to what is frequently assumed, the $Ar(1s_2)$ resonant state has the largest share in quenching reactions, due to the large values of $g_2/g = 0.4$ and $k_{Q,N_{2,2}}$ as shown in Table 1.

From known densities $\underline{n}_{Ar(1s_i)}$, N-atom densities achievable in the Ar–N_2 DBD can be calculated. With the three-body recombination reaction R2 as the dominant loss channel of nitrogen atoms[24][2]

$$2\,N + Ar \rightarrow N_2 + Ar \quad k_2 = 1.15 \times 10^{-32}\ cm^6/s, \quad (R2)$$
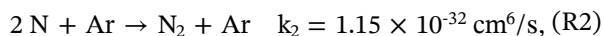
the rate equation and boundary condition (BC) for the density of N atoms, $n_N(t)$, generated in an Ar–N_2 mixture passing through the DBD zone by reaction R1 with rate coefficient k_1, and its solutions are expressed as follows:

$$dn_N/dt = g_N - 2k_2 n_0\, n_N^2 = 2k_1 n_{Ar(1s_i)} n_{N_2}$$
$$- 2k_2 n_0\, n_N^2;\quad BC:\ n_N(0) = 0 \Rightarrow, \quad (1)$$

$$n_N(t) = n_N(\infty) \tanh\left(\sqrt{4 \times k_1 n_{Ar(1s_i)} n_{N_2} \times k_2 n_0} \times t\right), \quad (2)$$

$$n_N(\infty) = \sqrt{k_1 n_{Ar(1s_i)} n_{N_2}/(k_2 n_0)}, \quad (3)$$

$$n_N(t \to 0) = 2 \times k_1 n_{Ar(1s_i)} n_{N_2} \times t. \quad (4)$$

---

[2]$k_2 \equiv -dn_N/dt/(2n_N^2\, n_0)$.

g_N in Equation 1 is the rate at which N atoms are produced by reaction R1, $n_0 = p/kT = 2.41 \times 10^{19}\ cm^{-3}$ at $T = 300$ K and $p = 1$ bar.

As shown in Section 3, Equation 4 allows to derive upper limits for the values of k_1 for generation of N atoms by energy transfer from Ar atoms in the resonant states $1s_2$ and $1s_4$.

3 | EXPERIMENTAL SECTION

Experiments were performed in an afterglow tube with 1.06-cm inner diameter, fed by a coaxial DBD arrangement as described in more detail earlier,[25] using pure N_2 and an Ar–N_2 mixture with 0.1% N_2 at a flow rate of 40 L/min STP (slm). A fraction of $x_{N_2} = 0.1\%$ was chosen as a compromise to have negligible effects of N_2 on the electron energy distribution function and low dissociation of N_2 by direct electron collisions with N_2, and to enable a significant energy transfer from $Ar(1s_i)$ to N_2 (see Figure 1). The discharge was powered by an HV generator 7020 Uz from Softal Electronics GmbH (Hamburg, Germany) operating at a frequency of 29 kHz. The plasma zone geometry was defined by an inner glass tube with 0.15-cm wall thickness and an outer radius of 0.75 cm, filled with copper powder as a high-voltage electrode, and an outer glass tube with the same wall thickness and an inner radius of 0.95 cm, covered over a length of 5 cm with an aluminum foil as a ground electrode, resulting in a gap width d of 0.2 cm and a plasma volume of 5.34 cm^3. The residence time in the discharge, τ_D, was 8.0 ms, and the average flow velocity in the afterglow tube was 755 cm/s.

For the measurement of voltages and (using a precision series resistor) currents, a TDS2012C oscilloscope from Tektronix (Beaverton, OR) was applied. Peak driving voltages and average discharge power densities, P_V, were 15 kV/6.3 W/cm^3 (N_2) and 11 kV/5.5 W/cm^3 (Ar-0.1% N_2), respectively. Optical emission spectra were measured using a QE65000 high-sensitivity fiber-optic spectrometer from Ocean Optics B. V. (EW Duiven, The Netherlands). Measurements were performed without a slit, and the diameter of the optical fiber used to couple the light into the spectrometer was 100 µm.

Figure 2 shows the optical emission of the N_2 afterglow taken at a position corresponding to an afterglow residence time, τ_A, of 9.3 ms. The spectrum shows bands of the First Positive System (FPS) of N_2, generated by a recombination of $N(^4S)$ atoms. A measurement under comparable conditions with the mixture of argon with 0.1% N_2 does not reveal any FPS bands. Considering the signal-to-noise ratio (SNR) of the 580-nm band in Figure 2 of about 100, one can conclude that the FPS
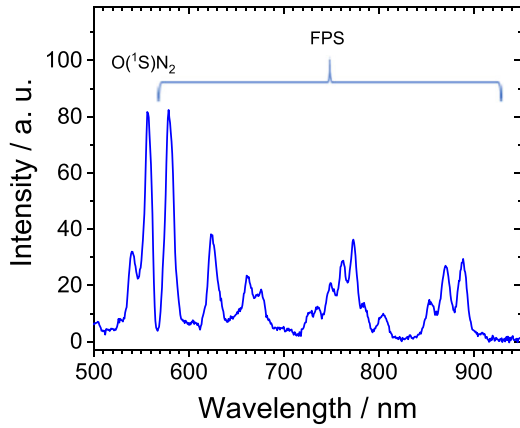
FIGURE 2 Optical emission spectrum of the dielectric-barrier discharges afterglow in pure N_2, at a position 7 cm downstream from the discharge ($\tau_A = 9.3$ ms). The spectrum shows components of the FPS of N_2 with a dominating band at 578 nm due to the transitions $N_2(B,11) \rightarrow N_2(A,7)$ and the band of the $O(^1S) \cdot N_2$ excimer at 557 nm. Further FPS bands can be seen at (in nm) 540 ($\Delta v = 5$); 624, 661, 670, 676 ($\Delta v = 3$); 727, 736, 749, 761, 773 ($\Delta v = 2$); and 805, 854, 871, 889 ($\Delta v = 1$). It should be noted that these band maxima can differ by up to 3 nm from the band head data in the monography by Pearse and Gaydon[26]

intensity due to the presence of any N atoms in an afterglow in Ar with 0.1% N_2 would be at least about a factor 50 smaller than in the N_2 afterglow if a SNR of 2 would be required for a signal to be detectable.

4 | CALCULATION OF N-ATOM DENSITY FROM POWER DENSITY IN THE DISCHARGE ZONE

The N-atom density in the N_2 afterglow can be calculated from the average DBD power density, P_V, and residence times in the discharge and the afterglow, τ_D and τ_A, respectively, using the equation:

$$
\begin{aligned}
n_N(\tau_D, \tau_A)/\text{cm}^{-3} \\
= [[1.93 \times 10^{14} \sqrt{P_V/\text{Wcm}^{-3}} \tanh(140\sqrt{P_V/\text{Wcm}^{-3}} \times \tau_D/\text{s})]^{-1} \\
+ 7.23 \times 10^{-13} \times \tau_A/\text{s}]^{-1}.
\end{aligned} \quad (5)
$$

τ_D is calculated from the entry of the gas into the discharge and τ_A from the entry into the afterglow region. The expression in the inner square bracket is the N-atom density $n_N(\tau_D)$ achieved in the gas phase after its passage through the discharge zone in which the power per volume P_V is dissipated. The hyperbolic tangent function results from the solution (Equation 7) of the differential equation and boundary condition in Equation (9) for power-density-proportional generation of N atoms ($g_N = \alpha \times P_V$) and decay by three-body recombination

(α^{-1} is the energy that has to be deposited in the gas to generate one N atom). Alternatively, the achieved N-atom density can be expressed as a function of the energy deposited per volume $\varepsilon_{V,D} = P_V \times \tau_D$:

$$
dn_N/dt = \alpha P_V - 2k_2 n_0 \, n_N^2; \quad \text{BC: } n_N(0) = 0, \quad (6)
$$

$$
n_N(\tau_D) = \sqrt{\alpha P_V/(2k_2 n_0)} \tanh\left(\sqrt{\alpha P_V \times 2k_2 n_0} \times \tau_D\right), \quad (7)
$$

$$
n_N(\varepsilon_{V,D}) = \sqrt{\alpha P_V/(2k_2 n_0)} \tanh\left(\sqrt{\alpha 2k_2 n_0/P_V} \times \varepsilon_{V,D}\right), \quad (8)
$$

where n_0 is $p/kT = 2.41 \times 10^{19}$ cm^{-3} at $T = 300$ K and $p = 1$ bar.

The factors in front of the square roots in Equation 5 were determined from experimental results reported by Es-Sebbar et al.[27] by fitting a hyperbolic tangent function to the data in fig. 11 of Reference [27], measured by 2-photon absorption laser-induced fluorescence spectroscopy. The curve fit results in the equation $n_N(\varepsilon_V) = 2.7 \tanh(\varepsilon_V/10/(10^{-3} \text{ J/cm}^3)) \times 10^{14}$ cm^{-3} (see Figure 3):

The energy density ε_V was varied by measuring at different positions and/or at different gas flows.[27] The figure shows an overlay of a copy of fig. 11 in Reference [27] and, in red color, the graph of the function given in the legend.

A comparison of this empirical equation with Equation 8 results in $\alpha = 2.70 \times 10^{16}$ J^{-1}, corresponding to "energy costs" of $\alpha^{-1} = 231$ eV per N atom. The recombination rate coefficient k_2 results as 1.5×10^{-32} cm^6/s; remarkably the same figure was suggested by Peeters et al.[2] as an average of reliable literature data.
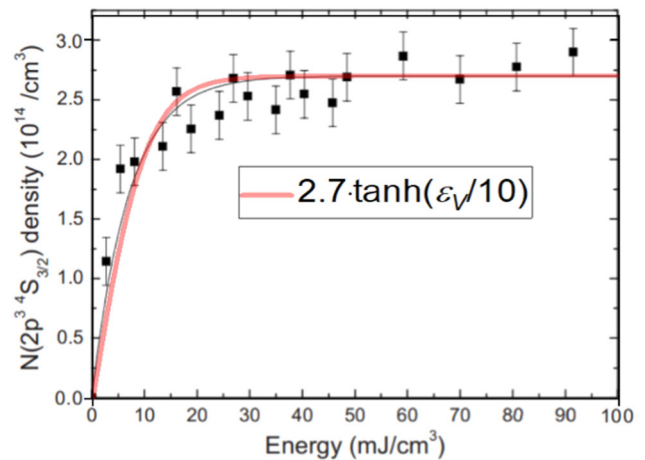

FIGURE 3 N-atom densities measured by Es-Sebbar et al. [27] in a filamentary dielectric-barrier discharge with a power density of $P_V = 2$ W/cm^3

The τ_A dependence in Equation 5 represents the loss of N atoms in the afterglow by way of three-body recombinations, with $n_N(\tau_D) = n_N(\tau_D, \tau_A = 0)$ playing the role of the initial value at $\tau_A = 0$. The equation can also be extended to account for wall losses, but in the present situation with relatively high N-atom densities, recombination losses are by far dominating, due to which wall losses were neglected.

5 | RESULTS AND DISCUSSION

Applied to the present experimental situation, Equation 5 yields N-atom densities, $n_N(8.0 \text{ ms}, 0) = 4.8 \times 10^{14} \text{ cm}^{-3}$ at the discharge end and $n_N(8.0, 9.3 \text{ ms}) = 1.1 \times 10^{14} \text{ cm}^{-3}$ at the OES measurement position in the afterglow.

Deriving an upper limit of the possible N-atom density in the afterglow with 0.1% N_2 in Ar, one has to take into account an intensification of FPS bands in the present situation, due to weaker quenching of $N_2(B, v')$ states in Ar.[28] Thus, the 580-nm band should be a factor of three more intensive in Ar with 0.1 % N_2 than in pure N_2 so that one can safely estimate that $n_N < 1 \times 10^{13} \text{ cm}^{-3}$ at the measurement position and, due to negligible recombination at that low density, also at the end of the discharge.

The absence of N-atom densities beyond $1 \times 10^{13} \text{ cm}^{-3}$ in the experiment with Ar containing 0.1% N_2 shows that the dissociation of N_2 after excitation of the molecule by energy transfer from any $Ar(1s_i)$ state cannot be an efficient process, if such a reaction takes place at all. If one excludes reactions with the two metastable Ar states as possible sources of N atoms, relying on the remark made in the publication by Setser et al.,[20] the resonant states are left as possible candidates in reaction R1. Owing to similar average densities of $Ar(1s_2)$ and $Ar(1s_4)$ under conditions of the measurement, $1.5 \times 10^{11} \text{ cm}^{-3}$, concerning the sum of the corresponding rate coefficients, one can conclude from Equation 4 that

$$(k_{1,2} + k_{1,4}) < 1 \times 10^{13}/(2 \times 1.5 \times 10^{11} \times 2.4 \times 10^{16}$$
$$\times 0.008) = 2 \times 10^{-13} \text{ cm}^3/\text{s}. \qquad (9)$$

Therefore, any reaction R1 with atoms in these states would have a rate coefficient two orders of magnitude below their total quenching rate coefficient (see Table 1). The dissociation of N_2 in reaction R1 will, therefore, generally be negligible if other channels leading to N atoms are available.

It is interesting to note that the dissociation of $N_2(X)$ into two $N(^4S)$ atoms cannot be achieved photochemically. UV photodissociation does not take place below a photon energy of $h\nu = 12.14 \text{ eV}$, and for $12.14 \text{ eV} \leq h\nu < 13.9 \text{ eV}$, the process results in $N(^4S) + N(^2D)$.[29] A dissociation

limit of 12.145 eV was already derived in the 1930s from spectroscopic investigations.[30] For dissociation of N_2 due to collisions with electrons, the formation of $N(^4S) + N(^2D)$ is the dominant dissociation mechanism; cross-sections for electrons of 10 and 12 eV energy are 0 and 10^{-18} cm^2, respectively. The formation of $N(^4S) + N(^4S)$ could not be excluded in the experiments but constitutes at the most a minor product channel.[31,32]

5.1 | Summary

The energy transfer from excited Ar atoms in 1s states to N_2 molecules is not an efficient source of nitrogen atoms. The sum of rate coefficients for dissociation of N_2 by reactions of atoms in $Ar(1s_2)$ and $Ar(1s_4)$ resonant states is less than $2 \times 10^{-13} \text{ cm}^3/\text{s}$, two orders of magnitude below the total quenching rates.

ORCID
Claus-Peter Klages http://orcid.org/0000-0001-5678-5845
Lars Bröcker http://orcid.org/0000-0002-7291-9265
Detlef Loffhagen http://orcid.org/0000-0002-3798-0773

REFERENCES
[1] U. Kogelschatz *Process Technologies for Water Treatment* (Ed: S. Stucki), Springer, Boston, MA **1988**, p. 87.
[2] F. J. J. Peeters, R. Yang, M. C. M. van de Sanden, *Plasma Sources Sci. Technol.* **2015**, *24*, 045006.
[3] A. Fridman, *Plasma Chemistry*, Cambridge University Press, UK, **2009**, pp. 5–3.
[4] A. Lofthus, P. H. Krupenie, *J. Phys. Chem. Ref. Data* **1977**, *6*, 113.
[5] A. V. Volynets, D. V. Lopaev, T. V. Rakhimova, A. A. Chukalovsky, Yu. A. Mankelevich, N. A. Popov, A. I. Zotovich, A. T. Rakhimov, *J. Phys. D: Appl. Phys.* **2018**, *51*, 364002.
[6] L. Minnhagen, *J. Opt. Soc. Am.* **1973**, *63*, 1185.
[7] U. Kogelschatz, *J. Opt. Technol.* **2012**, *79*, 484.
[8] J. E. Velazco, J. H. Kolts, D. W. Setser, *J. Chem. Phys.* **1978**, *69*, 4357.
[9] T. Oka, M. Kogoma, M. Imamura, S. Arai, T. Watanabe, *J. Chem. Phys.* **1979**, *70*, 3384.
[10] M. Moravej, X. Yang, M. Barankin, J. Penelon, S. E. Babayan, R. F. Hicks, *Plasma Sources Sci. Technol.* **2006**, *15*, 204.
[11] F. J. Gordillo-Vázquez, *J. Phys. D: Appl. Phys.* **2008**, *41*, 234016.
[12] T. Kimura, H. Kasugai, *J. Appl. Phys.* **2010**, *108*, 033305.
[13] M. N. Shneider, A. Baltuška, A. M. Zheltikov, *J. Appl. Phys.* **2011**, *110*, 083112.

[14] W. van Gaens, A. Bogaerts, *J. Phys. D: Appl. Phys.* **2013**, *46*, 275201.

[15] Y.-S. Liang, G.-H. Liu, C. Xue, Y.-X. Liu, Y.-N. Wang, *J. Appl. Phys.* **2017**, *121*, 203302.

[16] Y. Zhang, M. N. Shneider, R. B. Miles, *AIAA J.* **2018**, *56*, 1060.

[17] L. G. Piper, J. E. Velazco, D. W. Setser, *J. Chem. Phys.* **1973**, *59*, 3323.

[18] L. C. Pitchford, L. L. Alves, K. Bartschat, S. F. Biagi, M. C. Bordage, A. V. Phelps, C. M. Ferreira, G. J. M. Hagelaar, W. L. Morgan, S. Pancheshnyi, V. Puech, A. Stauffer, O. Zatsarinny, *J. Phys. D: Appl. Phys.* **2013**, *46*, 334001.

[19] C.-P. Klages, *Plasma. Processes Polym.* **2020**, e2000028. https://doi.org/10.1002/ppap.202000028

[20] D. W. Setser, D. H. Stedman, J. A. Coxon, *J. Chem. Phys.* **1970**, *53*, 1004.

[21] J. H. Kolts, H. C. Brashears, D. W. Setser, *J. Chem. Phys.* **1977**, *67*, 2931.

[22] C.-P. Klages, A. K. Czerny, J. Philipp, M. M. Becker, D. Loffhagen, *Plasma. Processes Polym.* **2017**, *14*, e1700081.

[23] M. M. Becker, T. Hoder, R. Brandenburg, D. Loffhagen, *J. Phys. D: Appl. Phys.* **2013**, *46*, 355203.

[24] W. Brennen, E. C. Shane, *J. Phys. Chem.* **1971**, *75*, 1552.

[25] Z. Khosravi, *Doctoral Thesis*, Technische Universität Braunschweig (Braunschweig, Germany) **2017**.

[26] R. W. B. Pearse, A. G. Gaydon, *The Identification of Molecular Spectra*, 4th ed., Chapman and Hall, London, GB **1976**, p. 218.

[27] E. Es-Sebbar, C. Sarra-Bournet, N. Naudé, F. Massines, N. Gherardi, *J. Appl. Phys.* **2009**, *106*, 073302.

[28] A. Ricard, J. Tétreault, J. Hubert, *J. Phys. B: At. Mol. Opt. Phys.* **1991**, *24*, 1115.

[29] O. Dutuit, N. Carrasco, R. Thissen, V. Vuitton, C. Alcaraz, P. Pernot, N. Balucani, P. Casavecchia, A. Canosa, S. Le Picard, J.-C. Loison, Z. Herman, J. Zabka, D. Ascenzi, P. Tosi, P. Franceschi, S. D. Price, P. Lavva, *Astrophys. J. Suppl. Ser.* **2013**, *204*, 20.

[30] G. Büttenbender, G. Herzberg, *Ann. Phys.* **1934**, *21*, 577.

[31] Y. Itikawa, *J. Phys. Chem. Ref. Data* **2006**, *35*, 31.

[32] P. C. Cosby, *J. Chem. Phys.* **1993**, *98*, 9544.